Sensors and Materials, Vol. 13, No. 5 (2001) 247–258
MYU Tokyo

S & M 0446

Understanding the Evolution of Silicon Surface Morphology during Aqueous Etching

Melissa A. Hines

Department of Chemistry, Cornell University, Ithaca, NY 14853

(Received September 1, 2000; accepted December 1, 2000)

Key words: silicon, ammonium fluoride, etching, STM

A combination of scanning tunneling microscopy (STM) experiments and kinetic Monte Carlo simulations have been used to measure the site-specific reactivity of Si(111) surfaces towards NH_4F etching. The observed reactivity is explained on the basis of a pentavalent transition state to oxidation. The effects of isopropanol (IPA) on etching have also been investigated. The morphological effects of IPA on silicon etching are attributed to the slow etching of the silicon isopropoxy species. A new method for the rapid assay of etchant anisotropy is also presented.

1. Introduction

For reasons that are not completely understood, the mechanical, chemical, and electronic properties of nanoscale structures are often strongly influenced by their surface and interface morphologies. For example, atomic-scale roughness of the Si/SiO_2 interface in a metal-oxide-semiconductor field effect transistor (MOSFET) gate can reduce the mobility of electrons in the channel by a factor of 4.[1] More recently, researchers at Cornell[2] have found that the quality or Q of nanoscale resonators (≈50–250 nm) is inversely proportional to their surface-to-volume ratio, which strongly suggests that surface effects play a major role in mechanical energy dissipation at this length scale. With these types of problems in mind, our research has been directed towards understanding and controlling the development of surface morphology during chemical etching — we are attempting to make "perfect" surfaces.

The chemical control of surface morphology is not an easy task, because etching and growth reactions occur primarily at defect sites, such as steps and kinks. Historically, the low density of these defect sites has rendered them "invisible" to surface probes, such as electronic (UPS, XPS) and vibrational (infrared, Raman, EELS) spectroscopies. To overcome these deficiencies, we have developed techniques to quantify the site-specific reactivity of defect sites, such as steps and kinks, using a combination of scanning tunneling microscopy (STM) measurements and kinetic Monte Carlo simulations. Measurements of site-specific reactivity have given us useful insights into the mechanisms of surface etching.

In a more general sense, the chemical origins of surface morphology are also poorly understood. Theories of chemical reactivity are based on local, atomic-scale considerations, such as steric hindrance, relative electronegativity and structural rigidity, which have an effective range of no more than a few nanometers. Surface morphology, on the other hand, develops over the course of many such reactions — tens or hundreds of monolayers may need to be removed to reach the final, steady-state morphology. Is the steady-state morphology, with its potentially long length scales, a simple consequence of the cumulative effect of many short-scale events, or do more subtle perturbations, such as strain, contamination or even random fluctuations, come to dominate the final morphology? We have begun to answer this question, both experimentally and theoretically.

Over the past five years, we have developed experimental and theoretical techniques to quantify the relationship between chemical reactivity and surface morphology, and we have used these techniques to investigate a number of morphological problems. For example, we have studied the control of short-range and long-range surface morphology[3,4] etching-induced morphological instabilities (etch hillocks)[5,6] and the chemical control of etchant anisotropy.[7] Perhaps our most interesting finding was that simple chemical etching can lead to morphologies that are much smoother than the thermodynamic limit.[4] During the course of these investigations, we developed a chemically realistic, kinetic Monte Carlo model of Si(111) surface etching,[8] new methodologies for the extraction of site-specific reaction rates from STM morphologies,[7] and a new technique for the rapid measurement of etchant anisotropy.[9] We have also developed a rapid screening technique for development of new etchants.

2. Extracting Site-Specific Reaction Rates from Etch Morphologies

STM is an outstanding probe of etching chemistry, because the etched surface morphology is itself a record of surface reactivity. As our experiments have shown,[5–7] reliable, site-specific reaction rates can be extracted from *ex situ* studies of the steady-state etched surface morphology using chemically realistic, kinetic Monte Carlo simulations. (Since aqueous silicon etching is exquisitely sensitive to contaminants — especially by metal ions — we prefer *ex situ* studies to *in situ* studies.) These experiments do not require a knowledge of the initial, unetched morphology, as they are performed in the steady-state etching regime.[8] In our first experiments, we showed that highly anisotropic etching reactions, which have site-specific reaction rates spanning many decades of reactivity, are

easily quantified with this technique.[5,6] More recently, we have shown that even relatively isotropic reactions, which do not give rise to characteristic etch features (*e.g.*, triangular pits), can be studied using a new method that we developed, which relies on kinetic competition with an etchant of known anisotropy.[7]

To date, we have concentrated on etched, H-terminated Si(111) surfaces. From a chemist's perspective, the Si(111) surface is almost ideal, because it has a large number of chemically distinct sites with structures that are known from previous, very detailed, spectroscopic studies.[10–13] These sites range from the very unreactive terrace site, which has an unstrained monohydride termination, to the highly distorted step $\langle \bar{1}\,\bar{1}\,2 \rangle$ site,* which has a dihydride termination, to the strained and distorted monohydride-terminated kink site. Of course, the microelectronics industry revolves around Si(100), and we will extend our studies to this surface in the near future.

The key to these experiments is the atomistic, kinetic Monte Carlo (KMC) simulator of Si(111) etching that we developed.[8] Although silicon etching has been studied with STM by a number of groups,[14–17] reliable site-specific reaction rates cannot be obtained from simple, mean field kinetics. Our large-scale ($\approx 10^6$ atoms), chemically realistic simulations allow us to directly compare experiment and theory and extract meaningful kinetic parameters. Our model incorporates the full structure of the Si(111) lattice, including the interlayer stacking pattern, and all possible reaction sites within the solid-on-solid approximation. The surface sites are classified according to their structure into seven chemically distinct species. During the simulation, single atoms are randomly removed from the surface according to user-specified, site-specific etch rates. Using an iterative process, these rates are adjusted until the experimental surface morphologies are satisfactorily reproduced.

3. The Chemistry of Ultraflat Surfaces: Site-Specific Etching of NH_4F/Si(111)

The technological potential and intellectual allure of chemical etching are captured in the three morphologies displayed in Fig. 1. The very rough morphology in Fig. 1(a) is representative of a well-annealed Si/SiO_2 interface formed on a polished Si(111) wafer. Although mirror smooth to the naked eye, this interface is very rough on the atomic scale. In contrast, the near-perfect morphology in Fig. 1(b) is the result of simple, room-temperature chemical etching in an aqueous NH_4F solution. This etched surface is characterized by nearly straight vicinal steps and nearly perfect etched terraces. This perfection is marred by the presence of small etch pits. Interestingly, pits that are larger than ≈ 50 Å have a pronounced equilateral triangular shape which is illustrated by the (rare) giant pits seen in Fig. 1(c).

These images raise two important questions. First, what chemical mechanism is responsible for this perfection? Second, can we use chemistry to control surface morphology?

*We use the shorthand terminology "step site" to denote the sites that would terminate a straight step formed by miscutting a Si(111) surface towards the direction.

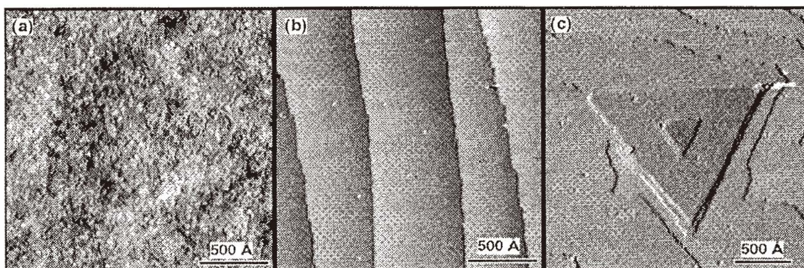

Fig. 1. STM images of etched Si(111). (a) Thermally oxidized Si(111) etched for 2 min in buffered HF (Transene) to remove oxide. The morphology reflects the original Si/SiO_2 interface. (b) Si(111) surface miscut in the $\langle 11\bar{2} \rangle$ direction and etched in 40% NH_4F (aq.) for 60 min in N_2 ambient. This surface is representative of our best preparations. (c) Si(111) surface miscut in the $\langle \bar{1}\bar{1}2 \rangle$ direction and etched in 40% NH_4F (aq.) Although the triple pit morphology is rare, all pits larger than ≈ 50Å have a pronounced equilateral triangular shape.

Like most aqueous etchants, NH_4F continuously removes silicon through sequential oxidation and etching reactions, which have been postulated to be:

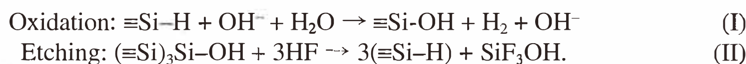

$$\text{Oxidation: } \equiv\text{Si–H} + OH^- + H_2O \rightarrow \equiv\text{Si-OH} + H_2 + OH^- \quad \text{(I)}$$
$$\text{Etching: } (\equiv\text{Si})_3\text{Si–OH} + 3HF \rightarrow 3(\equiv\text{Si–H}) + SiF_3OH. \quad \text{(II)}$$

As is usually the case for aqueous silicon etchants, oxidation is the rate-limiting step,[18] so the etched surfaces are unreconstructed and H-terminated.[10–13] The surface morphology is determined by the site-specificity of the rate-limiting reaction, Rxn. I.

The relative reactivities of Si(111) surface sites can be extracted from the steady-state etch morphology with the aid of kinetic Monte Carlo simulations. For example, the predominance of straight segments on the etched steps (Fig. 1(b)) is characteristic of a nucleation-propagation mechanism in which the etching of a step site is much slower than the etching of a kink site. Once a single atom is removed from the step (nucleation), two new kink sites will be created, and sequential kink etching or "unzipping" will proceed rapidly in a direction parallel to the step edge (propagation). The pronounced triangularity of the etch pits, which is illustrated by Fig. 1(c), can be explained by the relative reactivities of the two step types —the horizontal monohydride-terminated $\langle 11\bar{2} \rangle$ steps and the vertical dihydride-terminated $\langle \bar{1}\bar{1}2 \rangle$ steps which are illustrated in Fig. 2. The equilateral shape of these etch pits is the result of highly anisotropic step etching. Simulations show that the dihydride-terminated steps are 20 times more reactive than the monohydride-terminated steps.

By comparing our experimental morphologies with KMC simulations, we extracted the site-specific rates of NH_4F etching (i.e., Rxn I) from these steady-state morphologies. A comparison between our experimentally observed and simulated morphologies is shown in Fig. 3, while the kinetic parameters extracted from the simulations are illustrated in Fig. 2. Interestingly, even though all of the surface sites are silicon hydrides, the site-specific

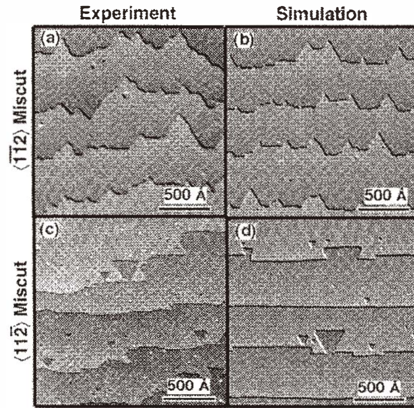

Fig. 2. The morphology of NH_4F-etched Si(111) surfaces and the best fit kinetic Monte Carlo simulations.

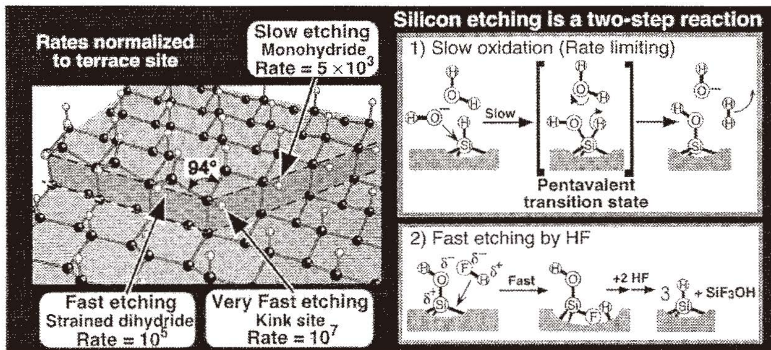

Fig. 3. Site-specific reactivities and mechanism of the etching of Si(111) by NH_4F (aq).

reactivities span a huge range — the strained and distorted kink site is 10^7 times more reactive than the flat terrace site!

The correlation between structure and reactivity provides important information about the mechanism of the rate-limiting reaction. In this case, the observed reactivities can be explained by the existence of a pentavalent transition state to H displacement as originally postulated by Hines *et al.*[19] In organosilicon chemistry, the displacement of a poor leaving group, such as H, from a silicon site is thought to proceed by bimolecular, front-side attack.[20-22] As a result, Si centers held in a rigid, tetrahedral environment react much more slowly than those held in less rigid or in distorted environments.

This proposed pentavalent transition state explains the relative reactivity of the kink, step and terrace sites. Sites that are held in a rigid, tetrahedral geometry by three bonds to the silicon substrate are difficult to distort. As a result, terrace and horizontal monohydride sites are relatively unreactive. On the other hand, sites that are already in a near-pentavalent geometry, such as the kink site, are highly reactive. The vertical dihydride lies in between these two extremes. Although this site is highly strained by steric interactions, the silicon center is nearly tetrahedral.[23] Because of this, the vertical dihydride is less reactive than the kink site, but more reactive than sites that are triply coordinated to the surface. Interestingly, unstrained dihydride sites, such as the point site, are more reactive than strained dihydrides. This observation is consistent with the proposed transition state and confirms the relative unimportance of bond strain in these reaction rates.

Detailed mechanistic information of this type will be useful in the development of new etchants with specific morphological properties.

4. Chemical Control of Surface Morphology: The Curious Effects of Isopropanol

Our analysis of NH_4F etching was based on the production of characteristic morphological features, such as triangular etch pits and shark's-tooth-shaped step edges, which are the direct consequence of highly anisotropic (i.e., site-specific) etching. We have recently shown that these techniques can be extended to much more isotropic etchants without the loss of chemical information.[7] To illustrate this, we studied the chemistry of a popular etch additive, isopropanol (IPA). This additive plays an important role in the production of microelectromechanical systems (MEMS), because it reduces undercutting by up to 75%[24,25] and leads to the production of very smooth etched surfaces.[26] Prior to our work, these morphological effects were attributed to surface tension; however, we have conclusively shown that they are actually due to surface chemistry.

To study IPA-enhanced etchants, we developed a new method for the quantification of surface defect reactivity of an essentially arbitrary chemical which is based on kinetic competition with an etchant of known, site-specific reactivity. The additive need not etch the surface directly. Binding of the additive to the etching surface produces a transient site blocking effect that perturbs the etched surface morphology. When the additive concentration is low, only highly reactive sites are blocked. As the additive concentration is increased, less reactive sites are also blocked. This effect leads to concentration-dependent changes in the etched surface morphology which can be related to the site-specific rates of additive binding and desorption/etching using kinetic Monte Carlo simulations.

The results of an experiment of this type are shown in Fig. 4, where the concentration-dependent effects of IPA on NH_4F etching are displayed. The site-specific rates of IPA binding (Rxn. III) and OH^- attack (Rxn. I) are highly correlated, as shown by Table 1, which strongly suggests that the reactions proceed through similar mechanisms. Nucleophilic displacement of hydrogen by alkoxide ions is well known in organosilicon chemistry.[27] Since this reaction is known to proceed through the same bimolecular, front-side attack mechanism as the OH^--mediated reaction,[20-22] we proposed that IPA reacts through

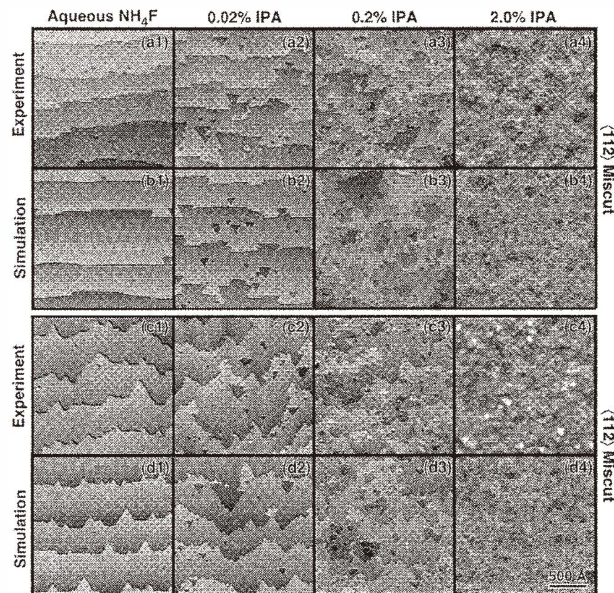

Fig. 4. Observed and simulated morphologies of Si(111) etched in IPA/NH_4F solutions. All simulations used the same site-specific reaction rates — only the initial miscut and IPA concentrations were changed.

Table 1
The site-specific rates of Rxns. I, III, and IV. c denotes the percentage of IPA (*e.g.*, c = 2 in 2% soln).

Site	NH_4F Etching (Rxn. I)	OR^- Attack (Rxn. III)	Si–OR Etching (Rxn. IV)
Kink	1	1 *c*	4×10^{-5}
Point	0.1	0.2 *c*	0.005
V Di	0.01	0.05 *c*	4×10^{-5}
H Mono	0.005	0.0005 *c*	4×10^{-5}
Terrace	10^{-7}	0	—

the analogous, sequential reactions

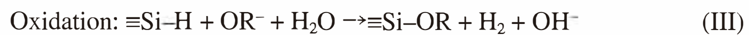

$$\text{Oxidation: } \equiv\text{Si–H} + OR^- + H_2O \rightarrow \equiv\text{Si–OR} + H_2 + OH^- \qquad \text{(III)}$$

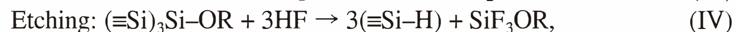

$$\text{Etching: } (\equiv\text{Si})_3\text{Si–OR} + 3HF \rightarrow 3(\equiv\text{Si–H}) + SiF_3OR, \qquad \text{(IV)}$$

where $R = CH(CH_3)_2$. The isopropoxide ion is relatively reactive and displaces H from silicon sites with essentially the same site-specificity as OH^- (Rxn. I). In contrast, etching of the silicon isopropoxy species (Rxn. IV) is slow and relatively isotropic. As a result, IPA-enhanced etchants are rate-limited by a slow, isotropic etching reaction (Rxn. IV), not by a fast, anisotropic oxidation (Rxn. III). This observation explains both the atomic-scale morphologies and (qualitatively) the changes in the macroscopic etch anisotropy.

5. A Rapid Screening Technique for Etchant Development

As we have shown, STM measurements can be combined with simulations to produce very detailed mechanistic information about etching reactions. Although these methods are very powerful, they are also very time-consuming and thus poorly suited to the development of new etchants. Fortunately, a full, atomic-scale investigation of every possible etchant is not necessary —only chemistries with new or unusual site-specific reactivities deserve this treatment. To complement our detailed atomic-level studies, we have developed a new method,[9] which relies on micromachined test patterns, to screen potential etch chemistries by their macroscopic etch anisotropies —their face-specific etch rates.

Although the macroscopic anisotropy cannot be inverted to obtain detailed atomic mechanisms, macroscopic etch rates do provide important clues to the underlying chemical reactions. For example, an etchant that produces atomically flat Si(100) surfaces must selectively etch all defect sites, while leaving the flat Si(100) surface virtually untouched. Macroscopically, this implies that the etchant must attack vicinal Si(100) surfaces, which are covered with atomic steps (i.e., defects), much more rapidly than flat Si(100) surfaces. In other words, a "perfect" etchant must be highly anisotropic with a pronounced etch rate minimum at the close-packed orientation. In contrast, an etchant that attacks all surfaces equally — an isotropic etchant — will presumably have little site specificity. Because of this correlation between the macroscopic etch rate and the microscopic reaction mechanism, etchant anisotropy can be used as a predictive indicator of atomic-scale morphologies.

Our technique is based on the geometric amplification inherent to the etching of wedges. When the sides of a wedge with an included angle α are etched by a distance Δt, the length of the wedge is reduced by a distance

$$\begin{aligned}\Delta l &= \Delta t \cot(\alpha/2) \\ &= 115\Delta t \text{ for } \alpha = 1°.\end{aligned}$$

In the case of alkaline silicon etchants, where etch rates are typically tens of microns per hour (at ≈ 70°C), the retraction rate of 1° wedges, which are easily produced using standard microfabrication techniques, is a few millimeters per hour — a distance easily seen by the naked eye and quantified with an optical microscope.

Our typical test pattern consists of 180 1°-wide wedges arranged in an evenly spaced, circular structure as conceptually diagrammed in Fig. 5(a). Each wedge is bounded by a different set of vertical planes, so the sides of each wedge etch with a characteristic, face-dependent rate. Anisotropic etching leads to the development of a characteristic "flower pattern," such as the one shown in Fig. 5(b). SEM micrographs of specific regions of etched and unetched structures are shown in Fig. 6. The flower pattern can be analyzed to yield absolute, face-specific etch rates. As a result, each experiment measures the absolute etch rate of 180 surfaces simultaneously.

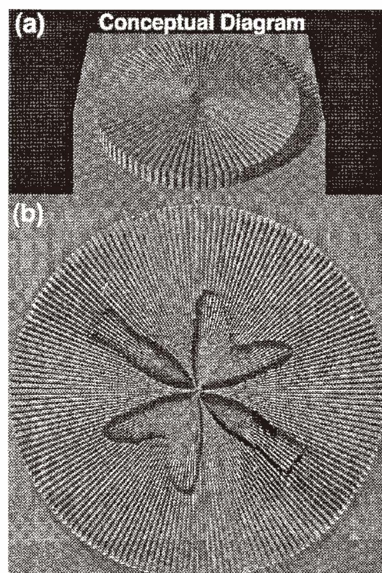

Fig. 5. The micromachined test structure. (a) Conceptual diagram of unetched structure, (b) optical micrograph of etch pattern formed by 70°C, 50% KOH (w/v). The structure is 16 mm in diameter, and each wedge is 1° wide.

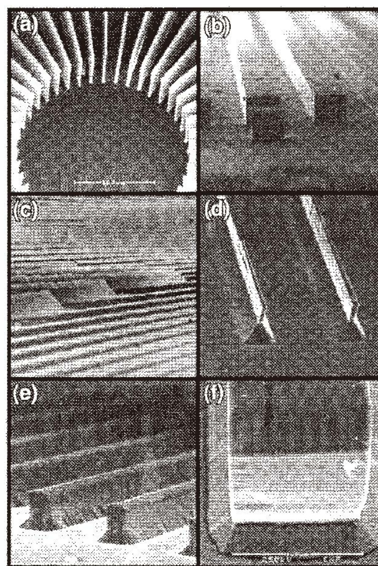

Fig. 6. SEM images of the micromachined pattern (a,b) before and (c-f) after etching. (a) Center region of pattern with 45 wedges showing vertical sidewalls. The wedges are ≈ 2 μm wide at their ends; (b) view of wedge ends and orientation marker. The wedges are 140 μm at their widest; (c) view of etched spokes near (100) minimum; (d) close-up of fast-etching spokes; (e) etched spokes showing formation of underetch structure at base; (f) close-up of etched spoke showing development of facets.

Figure 7 compares our measured etch rates in 50% KOH (w/v) with other values reported in the literature.[28,29] All of these data were obtained at 70°C. Since all three sets of data are in good agreement, we conclude that our new method is both accurate and precise.

These microfabricated structures can be used for two purposes. First, the etch pattern can be used as a simple screen for etch anisotropy, which would be useful for the development of new anisotropic etchants. Second, the pattern can be used to quantitatively compare similar etchants. For example, the reactivity of a series of alcohols, such as methanol, ethanol, and t-butanol, could be rapidly compared to isopropanol. If all of these etchants were to display similar absolute etch rates and anisotropies, we might conclude that further atomic-scale investigations were unwarranted.

6. Conclusions

The morphology of etched Si(111) surfaces can be explained by simple, site-specific reaction kinetics. Atomically flat surfaces are the result of highly anisotropic chemical reactions that specifically target defect sites, such as kinks. Etch additives, such as isopropanol, may alter etched surface morphologies by selectively binding to specific sites on the etched surface.

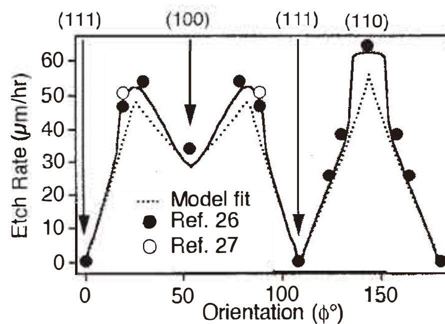

Fig. 7. Measured orientation-dependent etch rates in 70°C 50% KOH (w/v) (solid line) and best fit to simple model (dotted line). Rates measured by Sato *et al.*[28] (filled circles) and Herr and Baltes[29] (hollow circles) are shown for comparison.

Acknowledgments

This work was performed in collaboration with Y.-C. Huang, J. Flidr, T. A. Newton, R. A. Wind and L. A. Lepak. Support of this work by the Beckman Young Investigator program and the Petroleum Research Foundation is gratefully acknowledged. MAH is a Cottrell Scholar of the Research Corporation. This material was supported in part by the NSF under Award No. CHE-9733165 and by the MRSEC Program of the NSF under Award No. DMR-9632275.

References

1 T. Ohmi, K. Kotani, A. Teramoto and M. Miyashita: IEEE Electron Dev. Lett. **12** (1991) 652.
2 D. W. Carr, S. Evoy, L. Sekaric, J. M. Parpia and H. G. Craighead: Appl. Phys. Lett. **75** (1999) 920.
3 Y.-C. Huang, J. Flidr, T. A. Newton and M. A. Hines: J. Chem. Phys. **109** (1998) 5025.
4 Y.-C. Huang, J. Flidr, T. A. Newton and M. A. Hines: Phys. Rev. Lett. **80** (1998) 4462.
5 J. Flidr, Y.-C. Huang, T. A. Newton and M. A. Hines: Chem. Phys. Lett. **302** (1999) 85.
6 J. Flidr, Y.-C. Huang and M. A. Hines: J. Chem. Phys. **111** (1999) 6970.
7 T. A. Newton, Y.-C. Huang, L. A. Lepak and M. A. Hines: J. Chem. Phys. **111** (1999) 9125.
8 J. Flidr, Y.-C. Huang, T. A. Newton and M. A. Hines: J. Chem. Phys. **108** (1998) 5542.
9 R. A. Wind and M. A. Hines: Surf. Sci. **460** (2000) 21.
10 V. A. Burrows, Y. J. Chabal, G. S. Higashi, K. Raghavachari and S. B. Christman: Appl. Phys. Lett. **53** (1988) 998.
11 G. S. Higashi, Y. J. Chabal, G. W. Trucks and K. Raghavachari: Appl. Phys. Lett. **56** (1990) 656.
12 P. Jakob and Y. J. Chabal: J. Chem. Phys. **95** (1991) 2897.
13 M. A. Hines, Y. J. Chabal, T. D. Harris and A. L. Harris: Phys. Rev. Lett. **71** (1993) 2280.
14 J. J. Boland and J. H. Weaver: Physics Today **51**(8) (1998) 34.
15 R. S. Becker, G. S. Higashi, Y. J. Chabal and A. J. Becker: Phys. Rev. Lett. **65** (1990) 1917.
16 H. E. Hessel, A. Feltz, M. Reiter, U. Memmert and R. J. Behm: Chem. Phys. Lett. **186** (1991) 275 .
17 G. J. Pietsch, U. Köhler and M. Henzler: J. Appl. Phys. **73** (1993) 4797.
18 The macroscopic rate of silicon removal is linearly dependent on [OH^-] and independent of [HF]. T. A. Newton, Ph.D. Dissertation, Cornell University (2000).
19 M. A. Hines, Y. J. Chabal, T. D. Harris and A. L. Harris: J. Chem. Phys. **101** (1994) 8055.
20 L. H. Sommer: Stereochemistry, Mechanism and Silicon (McGraw-Hill, New York, 1965).
21 E. G. Rochow: in Comprehensive Inorganic Chemistry, edited by J. C. Bailar, Jr., H. J. Emeléus, and R. Nyholm (Pergamon, Oxford, 1973) **1** p. 123.
22 D. A. Armitage: Organosilanes in Comprehensive Organometallic Chemistry, ed. G. Wilkinson (Pergamon, Oxford, 1982) **2** p. 1.
23 K. Raghavachari, P. Jakob and Y. J. Chabal: Chem. Phys. Lett. **206** (1993) 156.
24 B. Puers and W. Sansen: Sensors and Actuators A **21–23** (1990) 1036.
25 A. Merlos, M. Acero, M. H. Bao, J. Bousells and J. Esteve: Sensors and Actuators A **37–38** (1993) 737.
26 S. A. Campbell, K. Cooper, L. Dixon, R. Earwaker, S. N. Port and D. J. Schiffrin: J. Micromech. Microeng. **5** (1995) 209 .
27 R. J. P. Corriu and C. Guerin: Adv. Organometal. Chem. **20** (1982) 265.

28 K. Sato, M. Shikida, Y. Matsushima, T. Yamashiro, K. Asaumi, Y. Iriye and M. Yamamoto: Sensors and Actuators A **64** (1998) 87.

29 E. Herr and H. Baltes: Sensors and Actuators A **31** (1992) 283.